EurJIC
European Journal of Inorganic Chemistry

Full Papers
doi.org/10.1002/ejic.202100342

Chemistry Europe
European Chemical Societies Publishing

Functional Group Variation in *tert*-Butyldiphenylsilanes (TBDPS): Syntheses, Reactivities, and Effects on the Intermolecular Interaction Pattern in the Molecular Crystalline State

Jonathan O. Bauer,*[a] Noel Angel Espinosa-Jalapa,[a] Nicolò Fontana,[a] Tobias Götz,[a] and Alexander Falk[a]

We present the preparation of *tert*-butyldiphenylsilanes differing in one functional group. The molecular structures of the phenyl (**3**), methoxy (**4**), and amino derivatives (**5**) were elucidated by single-crystal X-ray diffraction analysis and their crystal packing investigated by Hirshfeld surface analysis along with 2D fingerprint plots. In the all-*C* derivative **3**, the high symmetry dependence of the crystal packing enables a multitude of directional C(methyl)–H···C(π) interactions between the *tert*-butyl and phenyl groups. The methoxy derivative **4** is characterized by considerably short H···H contacts possibly resulting from pre-orienting C(aryl)–H···O and C(aryl)–H···C(π) hydrogen bonds. In the amino derivative **5**, the nitrogen atom is not involved in intermolecular interactions, instead dispersive H···H contacts might become more important for the crystal cohesion. These findings once again underline the pronounced lone electron pair density transfer from the nitrogen atom towards the silicon atom.

Introduction

Chloro-, methoxy-, and amino-functionalized silanes represent fundamentally important classes of compounds of considerable preparative interest.[1] They are commonly used as surface silylation reagents,[2] in protecting group chemistry,[3] and for the provision of silanes with special functional and reactive pattern.[4] Small molecules that only differ in specific functional groups are interesting model compounds to investigate both the suitability of certain functional groups for targeted transformations and the influence of heteroatoms on intra- and intermolecular structural parameters in the crystalline state.[5] This can also provide useful information for understanding structure-reactivity relationships and for building more complex functional molecular crystalline frameworks.[6] We recently reported on the synthesis of monofunctionalized disiloxane building blocks and their reactivity and chemoselectivity in further transformations.[7]

Driven by this previous study[7] and by our interest in structure-forming principles in molecular crystals,[8] we herein focus on silanes exhibiting a bulky and rigid *tert*-butyldiphenylsilyl (TBDPS) backbone (tBuPh$_2$Si–R, R = Cl, Ph, OMe, NC$_4$H$_8$). The TBDPS moiety is a widely used effective and bulky protecting group, as has already been impressively demonstrated in many organic syntheses,[9] and became an integral part of new catalyst designs.[10] Aryl-*tert*-butylfluorosilanes have gained medical importance as ^{18}F-labeled imaging agents in tumor diagnostics.[11] In recent years, the great importance of London dispersion interactions between polarizable aliphatic groups in molecular systems has been newly recognized[12] with implications on various areas of research.[13] The study of interactions that are generally considered weak is also of particular interest for a deeper understanding of the structure of molecular crystals. We therefore elaborated synthetic routes towards three single-crystalline *tert*-butyldiphenylsilanes that are either all-*C*-substituted (**3**: R = Ph) or exhibit a heteroatom function (**4**: R = OMe; **5**: R = NC$_4$H$_8$) (Scheme 1). The reactivity of the TBDPS derivatives towards lithiated regents was investigated. It was then of interest how the functional group variation effects the intermolecular interaction pattern in the molecular crystalline state.

Results and Discussion

tert-Butylchlorodiphenylsilane (**2**), prepared from dichlorodiphenylsilane (**1**) and *tert*-butyllithium, was chosen as adequate precursor for the convenient synthesis of the all-*C*- (**3**), methoxy- (**4**), and amino-functionalized (**5**) silanes (Scheme 1). Reaction of compound **2** with phenyllithium in hexane gave *tert*-butyltriphenylsilane (**3**) in good yield (72%). The methoxy- and *N*-pyrrolidinyl-substituted derivatives **4** and **5** were synthesized in isolated yields of 96% and 79%, respectively, by solvolysis of compound **2** using methanol/triethylamine or an

[a] Dr. J. O. Bauer, Dr. N. A. Espinosa-Jalapa, N. Fontana, T. Götz, A. Falk
Institut für Anorganische Chemie, Fakultät für Chemie und Pharmazie, Universität Regensburg
Universitätsstraße 31, 93053 Regensburg, Germany
E-mail: jonathan.bauer@ur.de

Supporting information for this article is available on the WWW under https://doi.org/10.1002/ejic.202100342

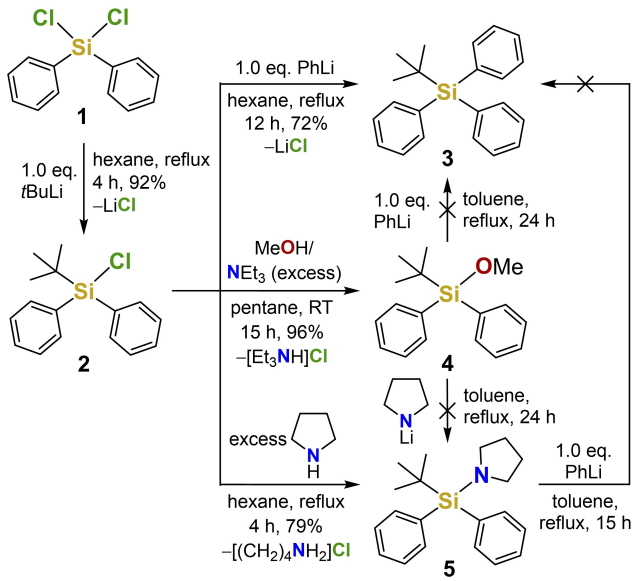

Scheme 1. Synthesis of model silanes **3**, **4**, and **5** starting from *tert*-butylchlorodiphenylsilane (**2**) to study structure-forming principles in the molecular crystalline state.

excess of pyrrolidine. An alternative procedure starting from compound **2** using the lithium amide in place of the amine gave compound **5** in 68% yield (see procedure **b** in the Experimental Section). In contrast to the chlorosilane (**2**), the methoxysilane (**4**) proved to be very inert towards nucleophilic attacks. The direct substitution of silicon-bound methoxy groups by lithium amides is known and the stability of the lithium methoxide by-product has been studied in detail,[1d] but neither compound **3** nor compound **5** could be obtained from methoxysilane **4** by direct nucleophilic substitution with the corresponding lithiated reagents, not even after heating at reflux in toluene for 24 hours.[14] It is becoming more and more evident that the reactivity of *tert*-butyl-substituted methoxysilanes towards nucleophilic attacks with lithiated reagents decreases dramatically as the degree of substitution increases, in sharp contrast to the respective chlorosilanes.[1d,4d] This is therefore not only due to the steric shielding of the silicon center, but also indicates differences in the substitution mechanism depending on the nature of the leaving group.[15] This reluctance of reactivity has recently also been observed for mesityl-substituted methoxysiloxanes.[7] In the case of a secondary carbon atom connected to silicon, a high reactivity can still be found for methoxytriorganosilanes, as the easy substitution reaction on a 2-(methoxydiphenylsilyl)pyrrolidine derivative with phenyllithium shows.[4c] Similar to the methoxysilane (**4**), heating a solution of the aminosilane (**5**) and phenyllithium at reflux in toluene for 15 hours showed no conversion to *tert*-butyltriphenylsilane (**3**) (Scheme 1).

The TBDPS group was found to have excellent crystallization properties for a variety of different R substituents. Compound **3** crystallized from dichloromethane/pentane at −30 °C in the trigonal crystal system, space group $P\bar{3}$ with a symmetry-dependent molecular structure ($Z' < 1$). Both compounds **4** and **5** crystallized from pentane at −30 °C in the triclinic crystal system, space group $P\bar{1}$ ($Z' = 1$) (Figure 1). Compounds **3**–**5** were then subjected to an in-depth study of their crystal packing with regard to weak intermolecular interactions by using state-of-the-art Hirshfeld surface analysis[16] and by analyzing the corresponding two-dimensional (2D) fingerprint diagrams.[17] The corresponding Hirshfeld surfaces and additional 2D fingerprint plots resoved in specific intermolecular contributions are shown in the Supporting Information.

Of all three compounds, the all-*C* derivative **3** shows the closest C···H/H···C contacts with a proportion of 26.4% (**4**: 21.2%, **5**: 17.0%). This is reflected by a considerable amount of symmetry-equivalent C(methyl)–H···C(π) interactions with closest contacts of 2.899 Å (H8A···C6) and 2.942 Å (H8B···C6), in which the methyl groups act as C–H donors pointing almost directly to a single π-bonded acceptor atom of a phenyl group (Figure 2). This kind of directionality is characterized by the spikes in the fingerprint diagram when it is resolved into C···H/H···C contributions (see the Supporting Information). For comparison, in *tert*-butylfluorodiphenylsilane,[11b] the shortes H···C contacts also use the *tert*-butyl group as C–H donor and can be attributed to edge-shifted C(methyl)–H···C(π) contacts, which, in addition to C–H···F–Si contacts, represent the most important directional interactions in the fluorine derivative. Although the C–H donor ability decreases in the series C(sp)–H > C(sp^2)–H > C(sp^3)–H,[18] aliphatic C–H groups are known to be significantly involved in stabilizing the crystal structure via attractive C–H···π interactions.[8c,19] Regarding the nature of the interaction, it was found that C–H···π interactions are dominated by dispersion rather than electrostatic contributions.[20]

The methoxy and amino derivatives **4** and **5** are quite different in their intermolecular interaction pattern from those of the phenyl analog **3** (Figure 1). Characteristic for the methoxysilane **4** is the pronounced central spike ($d_i = d_e \approx 1.1$ Å) (Figure 1, mid), which can be assigned to remarkably short H···H contacts between methoxy groups (H17A···H17A 2.305 Å) and between phenyl groups (H6···H6 2.354 Å) (see also the Supporting Information), which is in line with the generally accepted van der Waals radii of either 1.2 Å[21] or 1.1 Å[22] for hydrogen. Hydrogen···hydrogen contacts, which are still controversially discussed,[23] should be carefully considered when analyzing attractive intermolecular interactions in molecular crystals.[24] Even though the contribution of O···H/H···O contacts in compound **4** only amounts to 2.4%, they should not be neglected in their important directional role for the crystal packing due to their electrostatic nature.[18] The important role of this type of weak hydrogen bonds[25] has also recently been strengthened by the crystallographic analysis of the first ether solvate of hexaphenyldistannane.[8b] The shortest C–H···O contact is formed by the C3–H3 bond (H3···O 2.714 Å, C3···O 3.363 Å, C3–H3···O 126.01°) with H···O and C···O distances close to the sum of the van der Waals radii (Figure 3, left).[21,22] The H10···C5 contact of the edge-shifted C–H···π interaction, although not uncommonly short with 3.061 Å, might be an additional important anisotropic structure-defining contribution (for details concerning the directionality of this interaction, see also

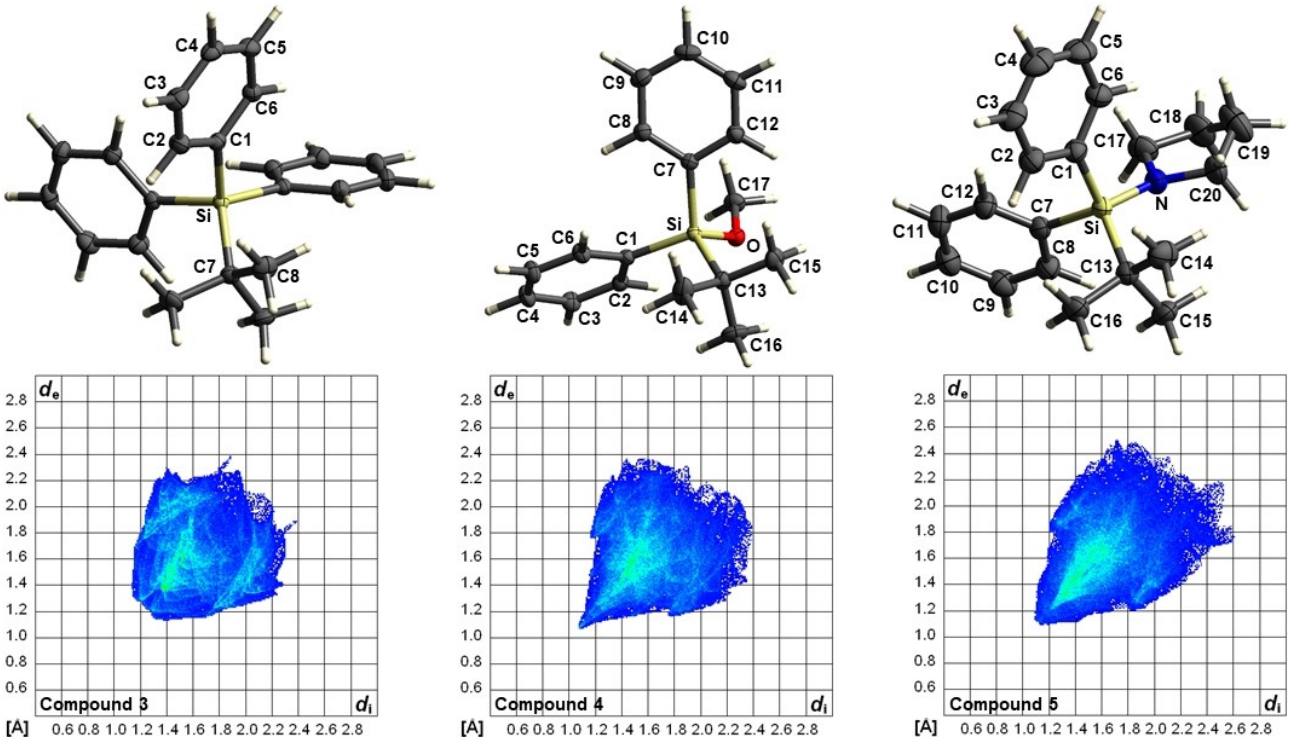

Figure 1. Molecular structures and 2D fingerprint plots (all contributions) of compounds **3**, **4**, and **5** in the crystal with the labeling scheme indicating the asymmetric unit (displacement ellipsoids set at the 50% probability level). Selected bond lengths [Å] and angles [°] of compound **3**: C1–Si 1.8794(10), C7–Si 1.9090(18), C6–C1–C2 116.98(10). Selected bond lengths [Å] and angles [°] of compound **4**: C1–Si 1.8769(14), C7–Si 1.8812(15), C13–Si 1.8889(16), O–Si 1.6457(10), C17–O 1.427(2), C6–C1–C2 116.93(13), C8–C7–C12 116.79(14), C17–O–Si 123.45(10). Selected bond lengths [Å] and angles [°] of compound **5**: C1–Si 1.877(2), C7–Si 1.881(2), C13–Si 1.904(2), N–Si 1.7266(17), C6–C1–C2 116.7(2), C8–C7–C12 117.08(19), C17–N–C20 109.70(19), C17–N–Si 121.74(15), C20–N–Si 125.41(18).

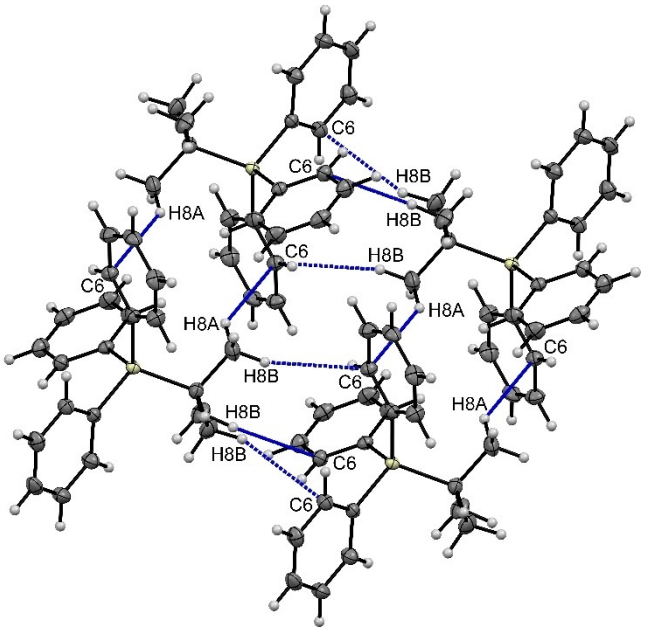

Figure 2. Part of the crystal structure of compound **3** illustrating short intermolecular distances in characteristic supramolecular synthon-like units (displacement ellipsoids set at the 50% probability level).

the Supporting Information). The molecular arrangement also causes a short H···H contact between phenyl groups (H2···H2 2.408 Å) (Figure 3, left). Since we expect the anisotropic C–H···O and C–H···C(π) contacts to be the strongest intermolecular interactions in the crystal structure of **4**, it can be assumed that the short H···H contacts result from a favorable molecular pre-orientation caused by C–H···O and C–H···π hydrogen bond-driven supramolecular synthon formation,[26] similar to the part of the crystal structure shown in Figure 3 (left). Compared to the previously and thoroughly investigated crystal structure of (1-naphthyl)trimethoxysilane,[8c] it becomes apparent that the anisotropic H···C and H···O contacts in compound **4** are less pronounced, but H···H interactions are all the more important.

When considering the *N*-pyrrolidinyl-substituted compound **5**, it is noticeable that the contribution of the nitrogen atom to C–H···N hydrogen bonding is rather neglectible with 0.2%. As in the methoxysilane **4**, the amino derivative **5** also has a relatively close C–H···π interaction (H5···C10 3.115 Å) of presumably structure-forming relevance (for details, see also the Supporting Information). Since the pyrrolidinyl group now serves with additional C–H bonds, the missing C–H···heteroatom hydrogen bonds in aminosilane **5** are apparently compensated by an increased number of isotropic H···H interactions (82.8%), the closest being found between H18B and H8 (2.318 Å) and between H18B and H17B (2.443 Å) (Figure 3, right). The N–Si

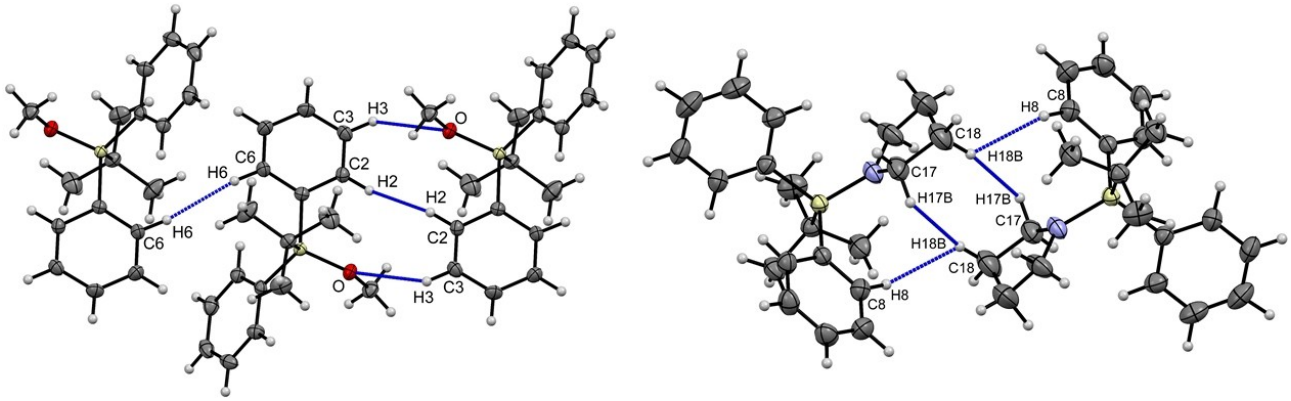

Figure 3. Part of the crystal structure of compounds **4** (left) and **5** (right) illustrating short intermolecular distances in characteristic supramolecular synthon-like units (displacement ellipsoids set at the 50 % probability level).

bond length [1.7266(17) Å] in **5** is a little longer than in pyrrolidinyl-substituted molecules with an NSiN[27] or NSiO[7,28] pattern. The planarization around the nitrogen atom [sum of angles: 356.9(5)°] is also somewhat less pronounced in **5**, which might be due to the missing interplay of lone electron pairs of two silicon–heteroatom bonds. Nevertheless, the delocalization of the lone-pair electron density that is typical for *N*-silylamines can also be seen here.[29] This is supported by the fact that the nitrogen atom is not to any significant extent involved in hydrogen bonding in the crystal structure.

Conclusions

In summary, we presented three single-crystalline *tert*-butyldiphenylsilanes that differ in one functional group. They can be viewed as simplified molecular model systems in order to elucidate straightforward transformations on bulky silanes and to reveal the effect of functional group variation on structure-forming principles in the molecular crystalline state. The methoxysilane **4** differs greatly from the chlorosilane precursor **2** in terms of its reactivity towards lithiated reagents. The analysis of the molecular crystal packing of the TBDPS-substituted compounds **3**–**5** gave detailed insights into the essential structure-forming interactions. Remarkably, the *tert*-butyl group is involved to a noteworthy extent in directional intermolecular interactions exclusively in the all-*C*-substituted compound **3**. C(methyl)–H···C(π) interactions are the most important structure-determining contacts in **3** and, due to the symmetry of the crystal structure, exist in large numbers. The methoxy and amino derivatives **4** and **5** both crystallize in the same space group. Anisotropic C–H···O and C–H···π interactions could play a key role in the pre-organization of supramolecular structural units in compound **4** with considerably short H···H contacts as a consequence. In silane **5**, the C–H···π and H···H contacts are generally somewhat widened due to the bigger heterocyclic substituent, and dispersive interactions owing to the increased number of C–H bonds are likely to play a greater role.

Studies on reactivity and chemoselectivity using specially functionalized molecular model systems provide valuable insight into functional group tolerance in reactions that are useful for preparative applications, e.g. for use as protecting groups in organic synthesis. Understanding the basic pattern of weak noncovalent interactions in the packing of molecular crystals can be of great importance for the design of functional molecular solids.

Experimental Section

General Remarks: All experiments were performed under an inert atmosphere of purified nitrogen by using standard Schlenk techniques. Glassware was heated at 140 °C prior to use. Hexane, pentane, and toluene were dried and degassed with a MBraun SP800 solvent purification system. *n*-Butyllithium (2.5 M solution in hexane, Merck KGaA), phenyllithium (1.9 M solution in dibutyl ether, Merck KGaA), dichlorodiphenylsilane (98 %, Merck KGaA), pyrrolidine (99 %, Merck KGaA), and triethylamine (99 %, Merck KGaA) were used without further purification. *tert*-Butylchlorodiphenylsilane (**2**),[1e,30] *tert*-butyltriphenylsilane (**3**),[31] and *tert*-butylmethoxydiphenylsilane (**4**)[30,32] have been reported previously. Benzene-d_6 used for NMR spectroscopy was dried over Na/K amalgam. NMR spectra were recorded on a Bruker Avance 400 spectrometer (400.13 MHz) at 25 °C. Chemical shifts (δ) are reported in parts per million (ppm). ^{1}H and ^{13}C{^{1}H} NMR spectra are referenced to tetramethylsilane ($SiMe_4$, $\delta = 0.0$ ppm) as external standard, with the deuterium signal of the solvent serving as internal lock and the residual solvent signal as an additional reference. ^{29}Si{^{1}H} NMR spectra are referenced to $SiMe_4$ ($\delta = 0.0$ ppm) as external standard. For the assignment of the multiplicities the following abbreviations were used: s = singlet, m = multiplet. High resolution mass spectrometry was carried out on a Jeol AccuTOF GCX and an Agilent Q-TOF 6540 UHD spectrometer. Elemental analyses were performed on a Vario MICRO cube apparatus.

X-ray Crystallography: Single-crystal X-ray diffraction analyses of compounds **3** and **4** were performed on an Oxford Diffraction CCD Xcalibur S diffractometer equipped with a Sapphire3 CCD detector at 173(2) K using graphite-monochromated Mo-Kα radiation ($\lambda =$ 0.71073 Å). Single-crystal X-ray diffraction analysis of compound **5** was performed on a SuperNova diffractometer equipped with a Atlas CCD detector at 123(1) K using Cu-Kα radiation ($\lambda =$

1.54184 Å). Data collection and reduction were performed using the CrysAlisPro software system, version 1.171.36.24 for **3** and **4**,[33a] and version 1.171.39.35c for **5**.[33b] The crystal structures were solved with SHELXT 2018/2 using Olex2.[34–36] The crystal structures were refined based on F^2 with the full-matrix least-squares method (SHELXL-2018/3)[36–38] using Olex2[35] and the SHELX program package as implemented in WinGX.[39] A multi-scan absorption correction using spherical harmonics as implemented in SCALE3 ABSPACK was employed.[33] The non-hydrogen atoms were refined using anisotropic displacement parameters. The hydrogen atoms were located on the difference Fourier map and refined independently. The Hirshfeld surfaces were mapped over d_{norm} ranging from 0.0480 to 1.2517 (**3**), −0.0361 to 1.1988 (**4**), and 0.0178 to 1.5694 a.u. (**5**). d_i and d_e in the 2D fingerprint diagrams are the distances from the surface to the nearest atom *interior* and *exterior* to the surface, respectively, and are each given in the range of 0.4 to 3.0 Å. The Hirshfeld surfaces and 2D fingerprint plots including Figure 1 and Figures S1–S6 in the Supporting Information were created using CrystalExplorer 17.5.[40] Figure 2 and Figure 3 were created using Mercury 4.1.0.[41]

Crystal Data and Structure Refinement of 3: Colorless blocks, 0.40×0.20×0.20 mm³, $C_{22}H_{24}Si$, Mr = 316.50 g·mol^{-1}, trigonal, space group (Nr.) $P\bar{3}$ (147), a = 11.4515(3) Å, b = 11.4515(3) Å, c = 7.8477(3) Å, V = 891.25(6) Å³, Z = 2, ρ = 1.179 g·cm^{-3}, μ = 0.130 mm^{-1}. 21651 reflections collected with Θ in the range 2.595–29.991°, index ranges $-15 \le h \le 16$, $-16 \le k \le 15$, $-10 \le l \le 10$, 1660 independent reflections (R_{int} = 0.0348), 102 parameters with 0 restraints gave final R indices $R1$ = 0.0357 and $wR2$ = 0.0932 [data with $I > 2\sigma(I)$]. $R1$ = 0.0422, $wR2$ = 0.0966 (all data), goodness-of-fit on F^2 = 1.081, largest electron density peak 0.385 $e \cdot$Å^{-3}, largest hole −0.226 $e \cdot$Å^{-3}.

Crystal Data and Structure Refinement of 4: Colorless blocks, 0.20×0.20×0.10 mm³, $C_{17}H_{22}OSi$, Mr = 270.43 g·mol^{-1}, triclinic, space group (Nr.) $P\bar{1}$ (2), a = 7.6146(4) Å, b = 9.6608(5) Å, c = 11.9962(7) Å, α = 111.072(5)°, β = 94.338(5)°, γ = 107.592(5)°, V = 767.92(8) Å³, Z = 2, ρ = 1.170 g·cm^{-3}, μ = 0.144 mm^{-1}. 18381 reflections collected with Θ in the range 2.383–29.866°, index ranges $-10 \le h \le 10$, $-13 \le k \le 13$, $-16 \le l \le 16$, 4009 independent reflections (R_{int} = 0.0372), 260 parameters with 0 restraints gave final R indices $R1$ = 0.0423 and $wR2$ = 0.0960 [data with $I > 2\sigma(I)$]. $R1$ = 0.0617, $wR2$ = 0.1049 (all data), goodness-of-fit on F^2 = 1.018, largest electron density peak 0.406 $e \cdot$Å^{-3}, largest hole −0.223 $e \cdot$Å^{-3}.

Crystal Data and Structure Refinement of 5: Clear colorless blocks, 0.44×0.30×0.11 mm³, $C_{20}H_{27}NSi$, Mr = 309.51 g·mol^{-1}, triclinic, space group (Nr.) $P\bar{1}$ (2), a = 9.9759(6) Å, b = 10.1439(5) Å, c = 10.1466(6) Å, α = 93.645(5)°, β = 116.927(6)°, γ = 93.863(4)°, V = 908.26(10) Å³, Z = 2, ρ = 1.132 g·cm^{-3}, μ = 1.092 mm^{-1}. 11264 reflections collected with Θ in the range 4.393–73.737°, index ranges $-11 \le h \le 12$, $-12 \le k \le 12$, $-12 \le l \le 12$, 3548 independent reflections (R_{int} = 0.0375), 307 parameters with 0 restraints gave final R indices $R1$ = 0.0552 and $wR2$ = 0.1491 [data with $I > 2\sigma(I)$]. $R1$ = 0.0594, $wR2$ = 0.1553 (all data), goodness-of-fit on F^2 = 1.082, largest electron density peak 0.692 $e \cdot$Å^{-3}, largest hole −0.526 $e \cdot$Å^{-3}.

Synthesis of *t*BuPh$_2$SiCl (2): *tert*-Butyllithium (25.0 mL of a 1.6 M solution in pentane, 40.0 mmol) was added dropwise to a solution of dichlorodiphenylsilane (**1**) (10.13 g, 40.0 mmol) in hexane (120 mL) at room temperature with stirring. The reaction mixture was then heated at reflux for 4 h. After cooling down to room temperature, the mixture was filtered through a fritted column layered with Celite® and the remaining solid washed with hexane (2×20 ml). The filtrates were collected and all volatiles removed *in vacuo*. The yellow oily residue was purified by Kugelrohr distillation (120 °C oven temperature, 1.2·10^{-1} mbar) to give compound **2** (10.11 g, 36.8 mmol, 92 %) as a pale-yellow oil. **^{1}H NMR** (400.13 MHz, C_6D_6): δ = 1.12 [s, 9H, C(CH_3)$_3$], 7.14 (m, 6H, H_{Ph}), 7.80 (m, 4H, H_{Ph}). **^{13}C{^{1}H} NMR** (100.62 MHz, C_6D_6): δ = 20.5 [s, C(CH$_3$)$_3$], 26.3 [s, C(CH$_3$)$_3$], 127.9 (s, C_{Ph}), 130.1 (s, C_{Ph}), 135.2 (s, C_{Ph}), 135.3 (s, C_{Ph}).

Synthesis of *t*BuPh$_3$Si (3): According to a modified procedure,[31] phenyllithium (3.8 mL of a 1.9 M solution in dibutyl ether, 7.3 mmol) was added dropwise to a solution of compound **2** (2.00 g, 7.3 mmol) in hexane (20 mL) at room temperature with stirring. The reaction mixture was then heated at reflux for 12 h. After cooling down to room temperature, the mixture was filtered through a fritted column layered with Celite® and the remaining solid washed with hexane (2×10 ml). The filtrates were collected, and all volatiles removed *in vacuo*. The remaining brownish oily residue was washed once with hexane (10 mL) to remove residual dibutyl ether yielding *t*BuPh$_3$Si (**3**) as a beige solid (1.66 g, 5.2 mmol, 72 %). Crystals suitable for single-crystal X-ray diffraction analysis were obtained from a concentrated dichloromethane solution layered with pentane at −30 °C within one week. **^{1}H NMR** (400.13 MHz, C_6D_6): δ = 1.20 [s, 9H, C(CH_3)$_3$], 7.16 (m, 9H, H_{Ph}), 7.68 (m, 6H, H_{Ph}). **^{13}C{^{1}H} NMR** (100.62 MHz, C_6D_6): δ = 18.9 [s, C(CH$_3$)$_3$], 29.0 [s, C(CH$_3$)$_3$], 128.1 (s, C_{Ph}), 129.5 (s, C_{Ph}), 135.2 (s, C_{Ph}), 136.9 (s, C_{Ph}). **^{29}Si{^{1}H} NMR** (79.49 MHz, C_6D_6): δ = −5.4 (s). **HRMS (FD+)**: $C_{22}H_{24}Si$ calcd. *m/z* for [M$^+$] 316.16418; found 316.16488. **CHN analysis**: $C_{22}H_{24}Si$ calcd. C 83.48 %, H 7.64 %; found C 82.43 %, H 7.77 %.

Synthesis of *t*BuPh$_2$SiOMe (4): According to a modified procedure,[30] methanol (5 mL) was added dropwise to a solution of compound **2** (2.75 g, 10.00 mmol) in pentane (10 mL) at −30 °C. Then, triethylamine (2 mL, 14.4 mmol) was added to the reaction mixture. The resulting white suspension was allowed to slowly warm up to room temperature and kept stirring for 15 h. Then, all volatiles were removed *in vacuo* and the residue extracted with pentane (3×20 mL). The extracts were collected and all volatiles removed *in vacuo* yielding compound **4** as a clear colorless oil, which crystallized on standing (2.60 g, 9.6 mmol, 96 %). Crystals suitable for single-crystal X-ray diffraction analysis were obtained from pentane at −30 °C overnight. **^{1}H NMR** (400.13 MHz, C_6D_6): δ = 1.13 [s, 9H, C(CH_3)$_3$], 3.38 (s, 3H, OCH_3), 7.20 (m, 6H, H_{Ph}), 7.74 (m, 4H, H_{Ph}). **^{13}C{^{1}H} NMR** (100.62 MHz, C_6D_6): δ = 19.4 [s, C(CH$_3$)$_3$], 27.0 [s, C(CH$_3$)$_3$], 52.0 (s, OCH$_3$), 128.1 (s, C_{Ph}), 129.9 (s, C_{Ph}), 134.0 (s, C_{Ph}), 135.9 (s, C_{Ph}). **^{29}Si{^{1}H} NMR** (79.49 MHz, C_6D_6): δ = −2.5 (s). **HRMS (FD+)**: $C_{17}H_{22}OSi$ calcd. *m/z* for [M$^+$] 270.14344; found 270.14411. **CHN analysis**: $C_{17}H_{22}OSi$ calcd. C 75.50 %, H 8.20 %; found C 75.35 %, H 8.41 %.

Synthesis of *t*BuPh$_2$Si(NC$_4$H$_8$) (5): Procedure (a): Pyrrolidine (5 mL) was added dropwise to a solution of compound **2** (2.75 g, 10.00 mmol) in hexane (10 mL) at room temperature. The resulting suspension was heated at reflux for 4 h. Then, all volatiles were removed *in vacuo* and the residue extracted with pentane (3×20 mL). The extracts were collected and all volatiles removed *in vacuo* yielding a beige oily residue. Recrystallization from pentane (10 mL) at −30 °C gave pure compound **5** as a beige crystalline material (2.44 g, 7.9 mmol, 79 %) over a period of three days. The crystalline material isolated as described was suitable for single-crystal X-ray diffraction analysis. **Procedure (b)**: *n*-Butyllithium (4.4 mL of a 2.5 M solution in hexane, 10.9 mmol) was added dropwise to a solution of pyrrolidine (776 mg, 10.9 mmol) in hexane (20 mL) at −30 °C. The resulting white suspension was then allowed to slowly warm up to room temperature and kept stirring for 1 h. A solution of compound **2** (2.50 g, 9.09 mmol) in hexane (20 mL) was added to the reaction mixture by means of a PTFE tube at room temperature. The resulting suspension was heated at reflux for 15 h. After cooling down to room temperature, the mixture was filtered through a fritted column layered with Celite® and the remaining solid washed with hexane (2×20 mL). The filtrates were

collected and all volatiles removed *in vacuo* yielding a beige oily residue. Recrystallization from pentane (10 mL) at −30 °C gave pure compound **5** as a beige crystalline material (1.91 g, 6.2 mmol, 68 %) over a period of three days. **^{1}H NMR** (400.13 MHz, C_6D_6): $\delta = 1.16$ [s, 9H, $C(CH_3)_3$], 1.56 (m, 4H, NCH_2CH_2), 3.06 (m, 4H, NCH_2CH_2), 7.22 (m, 6H, H_{Ph}), 7.71 (m, 4H, H_{Ph}). **^{13}C{^{1}H} NMR** (100.62 MHz, C_6D_6): $\delta = 19.8$ [s, $C(CH_3)_3$], 27.2 [s, $C(CH_3)_3$], 28.4 (s, NCH_2CH_2), 49.3 (s, NCH_2CH_2), 128.0 (s, C_{Ph}), 129.4 (s, C_{Ph}), 136.1 (s, C_{Ph}), 136.3 (s, C_{Ph}). **^{29}Si{^{1}H} NMR** (79.49 MHz, C_6D_6): $\delta = -7.9$ (s). **HRMS (EI+)**: $C_{20}H_{27}NSi$ calcd. *m/z* for [M^+] 310.1986; found 310.1987. **CHN analysis**: $C_{20}H_{27}NSi$ calcd. C 77.61 %, H 8.79 %, N 4.53 %; found C 77.40 %, H 8.74 %, N 4.44 %.

Deposition Numbers 2079905 (**3**), 2079906 (**4**), and 2079907 (**5**) contain the supplementary crystallographic data for this paper. These data are provided free of charge by the joint Cambridge Crystallographic Data Centre and Fachinformationszentrum Karlsruhe Access Structures service www.ccdc.cam.ac.uk/structures.

Acknowledgements

The Elite Network of Bavaria (ENB), the Bavarian State Ministry of Science and the Arts (StMWK), and the University of Regensburg are gratefully acknowledged for financial support (N-LW-NW-2016-366). In addition, we thank Prof. Dr. Manfred Scheer and Prof. Dr. Jörg Heilmann for generous and continuous support and excellent working conditions. Open access funding enabled and organized by Projekt DEAL.

Conflict of Interest

The authors declare no conflict of interest.

Keywords: Functionalization · Molecular model systems · Noncovalent interactions · Silanes · Structure elucidation

[1] a) M. A. Brook, *Silicon in Organic, Organometallic, and Polymer Chemistry*, John Wiley & Sons, New York, **2000**; b) U. Schubert, N. Hüsing, *Synthesis of Inorganic Materials* (4th Ed.), Wiley-VCH, Weinheim, **2019**; c) R. Wakabayashi, Y. Sugiura, T. Shibue, K. Kuroda, *Angew. Chem. Int. Ed.* **2011**, *50*, 10708–10711; *Angew. Chem.* **2011**, *123*, 10896–10899; d) J. O. Bauer, C. Strohmann, *Chem. Commun.* **2012**, *48*, 7212–7214; e) X. Fan, P. Xiao, Z. Jiao, T. Yang, X. Dai, W. Xu, J. D. Tan, G. Cui, H. Su, W. Fang, J. Wu, *Angew. Chem. Int. Ed.* **2019**, *58*, 12580–12584; *Angew. Chem.* **2019**, *131*, 12710–12714.

[2] a) T. Deschner, Y. Liang, R. Anwander, *J. Phys. Chem. C* **2010**, *114*, 22603–22609; b) S. P. Pujari, L. Scheres, A. T. M. Marcelis, H. Zuilhof, *Angew. Chem. Int. Ed.* **2014**, *53*, 6322–6356; *Angew. Chem.* **2014**, *126*, 6438–6474.

[3] P. G. M. Wuts, T. W. Greene, *Greene's Protective Groups in Organic Synthesis* (4th Ed.), John Wiley & Sons, Inc., Hoboken, **2006**.

[4] a) A. M. Muzafarov, E. A. Rebrov, *J. Polym. Sci. Part A* **2008**, *46*, 4935–4948; b) K. Igawa, N. Kokan, K. Tomooka, *Angew. Chem. Int. Ed.* **2010**, *49*, 728–731; *Angew. Chem.* **2010**, *122*, 740–743; c) J. O. Bauer, J. Stiller, E. Marqués-López, K. Strohfeldt, M. Christmann, C. Strohmann, *Chem. Eur. J.* **2010**, *16*, 12553–12558; d) J. O. Bauer, C. Strohmann, *Angew. Chem. Int. Ed.* **2014**, *53*, 720–724; *Angew. Chem.* **2014**, *126*, 738–742; e) P. Mizar, T. Wirth, *Angew. Chem. Int. Ed.* **2014**, *53*, 5993–5997; *Angew. Chem.* **2014**, *126*, 6103–6107; f) M. Herbig, U. Böhme, E. Kroke, *Z. Anorg. Allg. Chem.* **2019**, *645*, 377–387; g) M. Herbig, L. Gevorgyan, M. Pflug, J. Wagler, S. Schwarzer, E. Kroke, *ChemistryOpen* **2020**, *9*, 894–902; h) T. Lainer, M. Leypold, C. Kugler, R. C. Fischer, M. Haas, *Eur. J. Inorg. Chem.* **2021**, 529–533.

[5] a) D. Troegel, C. Burschka, S. Riedel, M. Kaupp, R. Tacke, *Angew. Chem. Int. Ed.* **2007**, *46*, 7001–7005; *Angew. Chem.* **2007**, *119*, 7131–7135; b) S. Metz, C. Burschka, D. Platte, R. Tacke, *Angew. Chem. Int. Ed.* **2007**, *46*, 7006–7009; *Angew. Chem.* **2007**, *119*, 7136–7139.

[6] a) J. L. Atwood, G. W. Gokel, L. J. Barbour, *Comprehensive Supramolecular Chemistry II* (2nd Ed.), Elsevier Ltd., Amsterdam, Oxford, Cambridge, **2017**; b) J. L. Atwood, L. J. Barbour, A. Jerga, *Science* **2002**, *296*, 2367–2369.

[7] N. A. Espinosa-Jalapa, J. O. Bauer, *Z. Anorg. Allg. Chem.* **2020**, *646*, 828–834.

[8] a) J. O. Bauer, *Z. Kristallogr. New Cryst. Struct.* **2020**, *235*, 353–356; b) J. O. Bauer, *Main Group Met. Chem.* **2020**, *43*, 1–6; c) J. O. Bauer, *Z. Anorg. Allg. Chem.* **2021**, *647*, 1053–1057; d) J. O. Bauer, T. Götz, *Chemistry* **2021**, *3*, 444–453.

[9] a) T. P. Brady, S. H. Kim, K. Wen, E. A. Theodorakis, *Angew. Chem. Int. Ed.* **2004**, *43*, 739–742; *Angew. Chem.* **2004**, *116*, 757–760; b) J. S. Clark, T. C. Fessard, C. Wilson, *Org. Lett.* **2004**, *6*, 1773–1776; c) G. Pattenden, N. J. Ashweek, C. A. G. Baker-Glenn, J. Kempson, G. M. Walker, J. G. K. Yee, *Org. Biomol. Chem.* **2008**, *6*, 1478–1497; d) B. Wang, T. M. Hansen, T. Wang, D. Wu, L. Weyer, L. Ying, M. M. Engler, M. Sanville, C. Leitheiser, M. Christmann, Y. Lu, J. Chen, N. Zunker, R. D. Cink, F. Ahmed, C.-S. Lee, C. J. Forsyth, *J. Am. Chem. Soc.* **2011**, *133*, 1484–1505; e) H. Xu, J.-P. Qu, S. Liao, H. Xiong, Y. Tang, *Angew. Chem. Int. Ed.* **2013**, *52*, 4004–4007; *Angew. Chem.* **2013**, *125*, 4096–4099; f) Y. Araki, A. Nakazaki, T. Nishikawa, *Org. Lett.* **2021**, *33*, 989–994.

[10] a) W. J. Drury III, N. Zimmermann, M. Keenan, M. Hayashi, S. Kaiser, R. Goddard, A. Pfaltz, *Angew. Chem. Int. Ed.* **2004**, *43*, 70–74; *Angew. Chem.* **2004**, *116*, 72–76; b) T. Hashimoto, Y. Kawamata, K. Maruoka, *Nat. Chem.* **2014**, *6*, 702–705.

[11] a) R. Schirrmacher, G. Bradtmöller, E. Schirrmacher, O. Thews, J. Tillmanns, T. Siessmeier, H. G. Buchholz, P. Bartenstein, B. Wängler, C. M. Niemeyer, K. Jurkschat, *Angew. Chem. Int. Ed.* **2006**, *45*, 6047–6050; *Angew. Chem.* **2006**, *118*, 6193–6197; b) G. Bradtmöller, K. Jurkschat, M. Schürmann, *Acta Crystallogr. Sect. E* **2006**, *62*, o1393-o1394; c) L. Iovkova, B. Wängler, E. Schirrmacher, R. Schirrmacher, G. Quandt, G. Boening, M. Schürmann, K. Jurkschat, *Chem. Eur. J.* **2009**, *15*, 2140–2147; d) H. Ilhan, S. Lindner, A. Todica, C. C. Cyran, R. Tiling, C. J. Auernhammer, C. Spitzweg, S. Boeck, M. Unterrainer, F. J. Gildehaus, G. Böning, K. Jurkschat, C. Wängler, B. Wängler, R. Schirrmacher, P. Bartenstein, *Eur. J. Nucl. Med. Mol. Imaging* **2020**, *47*, 870–880; e) S. Lindner, M. Simmet, F. J. Gildehaus, K. Jurkschat, C. Wängler, B. Wängler, P. Bartenstein, R. Schirrmacher, H. Ilhan, *Nucl. Med. Biol.* **2020**, *88–89*, 86–95.

[12] a) S. Grimme, R. Huenerbein, S. Ehrlich, *ChemPhysChem* **2011**, *12*, 1258–1261; b) S. Rösel, C. Balestrieri, P. R. Schreiner, *Chem. Sci.* **2017**, *8*, 405–410; c) S. Rösel, H. Quanz, C. Logemann, J. Becker, E. Mossou, L. Cañadillas-Delgado, E. Caldeweyher, S. Grimme, P. R. Schreiner, *J. Am. Chem. Soc.* **2017**, *139*, 7428–7431; d) S. Rösel, J. Becker, W. D. Allen, P. R. Schreiner, *J. Am. Chem. Soc.* **2018**, *140*, 14421–14432.

[13] a) J. Vondrášek, T. Kubař, F. E. Jenney, Jr., M. W. W. Adams, M. Kožíšek, J. Černý, V. Sklenář, P. Hobza, *Chem. Eur. J.* **2007**, *13*, 9022–9027; b) M. Kolář, T. Kubař, P. Hobza, *J. Phys. Chem. B* **2011**, *115*, 8038–8046; c) K. Fumino, V. Fossog, P. Stange, D. Paschek, R. Hempelmann, R. Ludwig, *Angew. Chem. Int. Ed.* **2015**, *54*, 2792–2795; *Angew. Chem.* **2015**, *127*, 2834–2837; d) C. Eschmann, L. Song, P. R. Schreiner, *Angew. Chem. Int. Ed.* **2021**, *60*, 4823–4832; *Angew. Chem.* **2021**, *133*, 4873–4882.

[14] A mixture of methoxysilane **4** and methyllithium in toluene showed no reaction at room temperature and led to only 30 % conversion after heating at reflux for 15 hours.

[15] L. H. Sommer, W. D. Korte, *J. Am. Chem. Soc.* **1967**, *89*, 5802–5806.

[16] M. A. Spackman, D. Jayatilaka, *CrystEngComm* **2009**, *11*, 19–32.

[17] M. A. Spackman, J. J. McKinnon, *CrystEngComm* **2002**, *4*, 378–392.

[18] a) T. Steiner, *Chem. Commun.* **1997**, 727–734; b) T. Steiner, G. R. Desiraju, *Chem. Commun.* **1998**, 891–892.

[19] a) Y. Kodama, K. Nishihata, M. Nishio, N. Nakagawa, *Tetrahedron Lett.* **1977**, *18*, 2105–2108; b) M. Nishio, Y. Umezawa, M. Hirota, Y. Takeuchi, *Tetrahedron* **1995**, *51*, 8665–8701; c) V. R. Thalladi, R. Boese, S. Brasselet, I. Ledoux, J. Zyss, R. K. R. Jetti, G. R. Desiraju, *Chem. Commun.* **1999**, 1639–1640; d) M. Nishio, *CrystEngComm* **2004**, *6*, 130–158; e) M. Nishio, Y. Umezawa, K. Honda, S. Tsuboyama, H. Suezawa, *CrystEngComm* **2009**, *11*, 1757–1788.

[20] a) A. Fujii, H. Hayashi, J. W. Park, T. Kazama, N. Mikami, S. Tsuzuki, *Phys. Chem. Chem. Phys.* **2011**, *13*, 14131–14141; b) J. W. G. Bloom, R. K. Raju, S. E. Wheeler, *J. Chem. Theory Comput.* **2012**, *8*, 3167–3174.

[21] A. Bondi, *J. Phys. Chem.* **1964**, *68*, 441–451.

[22] R. S. Rowland, R. Taylor, *J. Phys. Chem.* **1996**, *100*, 7384–7391.
[23] a) C. F. Matta, J. Hernández-Trujillo, T.-H. Tang, R. F. W. Bader, *Chem. Eur. J.* **2003**, *9*, 1940–1951; b) J. Poater, M. Solà, F. M. Bickelhaupt, *Chem. Eur. J.* **2006**, *12*, 2889–2895.
[24] a) A. M. Pendás, E. Francisco, M. A. Blanco, C. Gatti, *Chem. Eur. J.* **2007**, *13*, 9362–9371; b) J. Echeverría, G. Aullón, D. Danovich, S. Shaik, S. Alvarez, *Nat. Chem.* **2011**, *3*, 323–330; c) Á. Sánchez-González, A. Gil, *RSC Adv.* **2021**, *11*, 1553–1563; d) T. G. Bates, J. H. de Lange, I. Cukrowski, *J. Comput. Chem.* **2021**, *42*, e26491.
[25] a) G. R. Desiraju, *Acc. Chem. Res.* **1991**, *24*, 290–296; b) T. Steiner, *Angew. Chem. Int. Ed.* **2002**, *41*, 48–76; *Angew. Chem.* **2002**, *114*, 50–80.
[26] a) G. R. Desiraju, *Angew. Chem. Int. Ed. Engl.* **1995**, *34*, 2311–2327; *Angew. Chem.* **1995**, *107*, 2541–2558; b) G. R. Desiraju, *Angew. Chem. Int. Ed.* **2007**, *46*, 8342–8356; *Angew. Chem.* **2007**, *119*, 8492–8508; c) G. R. Desiraju, *J. Am. Chem. Soc.* **2013**, *135*, 9952–9967.
[27] S. Anga, Y. Sarazin, J.-F. Carpentier, T. K. Panda, *ChemCatChem* **2016**, *8*, 1373–1378.
[28] J. O. Bauer, C. Strohmann, *Organometallics* **2021**, *40*, 11–15.
[29] N. Kocher, C. Selinka, D. Leusser, D. Kost, I. Kalikhman, D. Stalke, *Z. Anorg. Allg. Chem.* **2004**, *630*, 1777–1793.
[30] R. Savela, W. Zawartka, R. Leino, *Organometallics* **2012**, *31*, 3199–3206.
[31] W. J. Vloon, J. C. van den Bos, N. P. Willard, G.-J. Koomen, U. K. Pandit, *Recl. Trav. Chim. Pays-Bas* **1991**, *110*, 414–419.
[32] T.-J. Du, Q.-P. Wu, H.-X. Liu, X. Chen, Y.-N. Shu, X.-D. Xi, Q.-S. Zhang, Y.-Z. Li, *Tetrahedron* **2011**, *67*, 1096–1101.
[33] a) CrysAlisPro Software System, *Agilent Technologies*, **2012**; b) CrysAlisPro Software System, *Rigaku Oxford Diffraction*, **2017**.
[34] G. M. Sheldrick, *Acta Crystallogr. Sect. A* **2015**, *71*, 3–8.
[35] O. V. Dolomanov, L. J. Bourhis, R. J. Gildea, J. A. K. Howard, H. Puschmann, *J. Appl. Crystallogr.* **2009**, *42*, 339–341.
[36] G. M. Sheldrick, *Acta Crystallogr. Sect. A* **2008**, *64*, 112–122.
[37] G. M. Sheldrick, *Acta Crystallogr. Sect. C* **2015**, *71*, 3–8.
[38] G. M. Sheldrick, *SHELXL-2018*, Universität Göttingen, Göttingen (Germany), **2018**.
[39] L. J. Farrugia, *J. Appl. Crystallogr.* **2012**, *45*, 849–854.
[40] M. J. Turner, J. J. McKinnon, S. K. Wolff, D. J. Grimwood, P. R. Spackman, D. Jayatilaka, M. A. Spackman, *CrystalExplorer17*, University of Western Australia, Perth (Australia), **2017**.
[41] C. F. Macrae, P. R. Edgington, P. McCabe, E. Pidcock, G. P. Shields, R. Taylor, M. Towler, J. van de Streek, *J. Appl. Crystallogr.* **2006**, *39*, 453–457.

Manuscript received: April 26, 2021
Revised manuscript received: May 20, 2021
Accepted manuscript online: May 25, 2021

FULL PAPERS

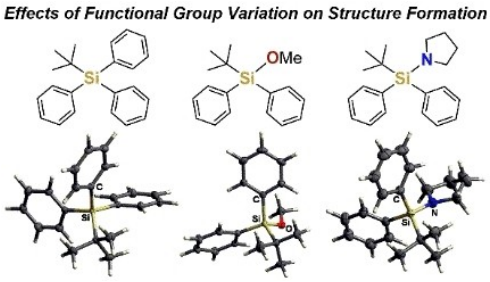

Functionalized small molecules that differ in only one functional group are useful molecular systems for model studies on reactivity and chemoselectivity. Straightforward synthetic routes towards three crystalline *tert*-butyldiphenylsilanes (TBDPS) are presented and their crystal packing is analyzed with regard to weak intermolecular interactions. This work contributes to our understanding of structure-forming principles in the molecular crystalline state.